**iScience, Volume *27***

## Supplemental information

# Type I interferon regulation by USP18 is a key vulnerability in cancer

**Veronica Jové, Heather Wheeler, Chiachin Wilson Lee, David R. Healy, Kymberly Levine, Erik C. Ralph, Masaya Yamaguchi, Ziyue Karen Jiang, Edward Cabral, Yingrong Xu, Jeffrey Stock, Bing Yang, Anand Giddabasappa, Paula Loria, Agustin Casimiro-Garcia, Benedikt M. Kessler, Adán Pinto-Fernández, Véronique Frattini, Paul D. Wes, and Feng Wang**

## Supplemental Information

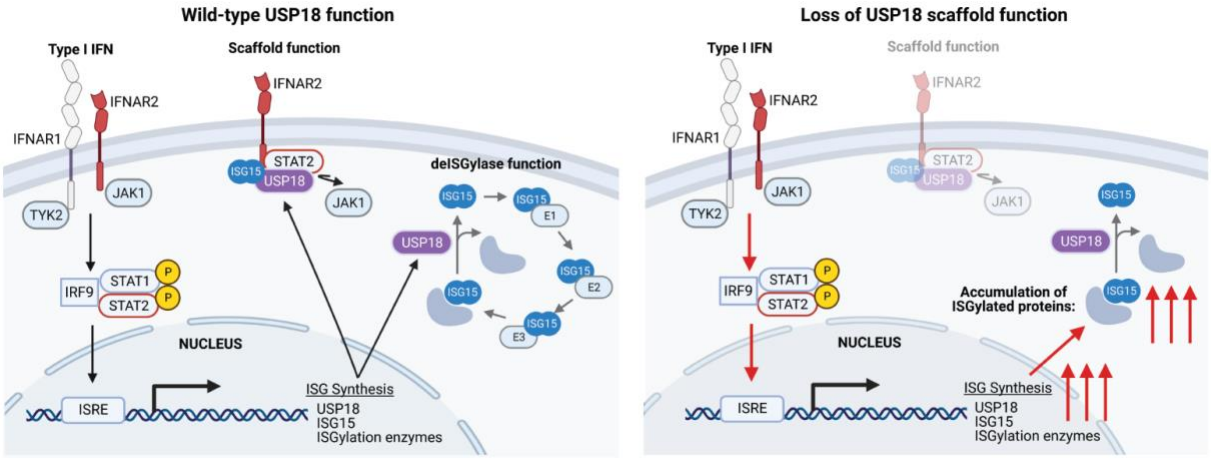


**Figure S1. Loss of USP18 scaffold function can increase ISG induction and ISGylated protein pool, related to Figure 1 and 4.** Type I IFN activation of the IFNAR signaling cascade results in ISG synthesis. Type I IFN-inducible ISGs include USP18, ISG15, and the enzymes required for ISGylation (UBA7, UBCH8/UBE2L6, and HERC5). USP18 negatively regulates IFN responses by displacing JAK1 to repress IFNAR signaling and removing ISG15 from ISGylated proteins (left schematic). Loss of USP18 scaffold function derepresses IFNAR signaling, resulting in hypersensitivity to Type I IFNs, increased ISG synthesis, and increased ISGylation of newly synthesized proteins (right schematic). Schematics created with BioRender.com.

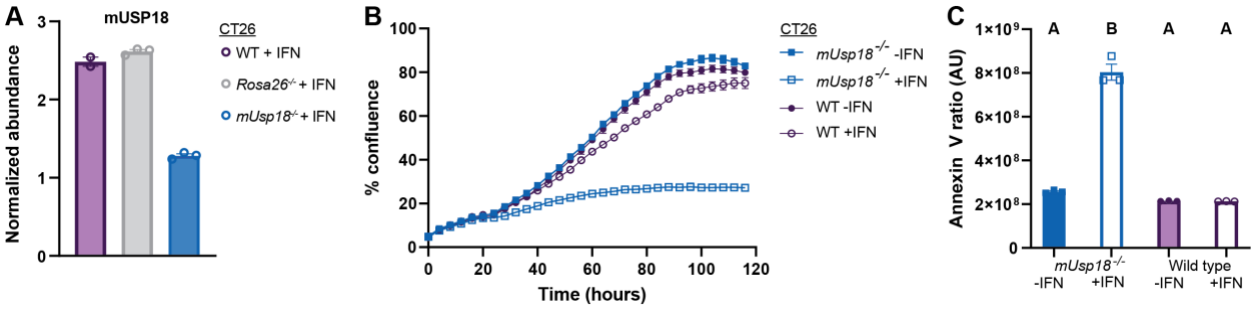


**Figure S2. IFN induces apoptosis in *mUsp18*$^{-/-}$ cells, related to Figure 1** Additional in vitro characterization *mUsp18*$^{-/-}$, *Rosa26*$^{-/-}$, and parental (WT) CT26 cancer cells prior to implantation in Figure 1A-C. (A) USP18 protein expression was assessed after 48 h treatment with 333 U/mL mouse IFN-β. Bottom-up mass spectrometry-based proteomics analysis was performed, with relative quantitation enabled by tandem mass tag labeling; n = 2 (WT) or 3 (*mUsp18*$^{-/-}$ and *Rosa26*$^{-/-}$) replicates per condition; mean ± SEM. (B,C) Growth rate (B) and viability (C) of WT and *mUsp18*$^{-/-}$ CT26 cancer cells ± 111 U/mL mouse IFN-α added at time = 0 hours. Each data point denotes n = 3 replicates; mean ± SEM. (C) Apoptotic cells at time = 112 h were detected by annexin V staining and normalized to total phase confluence to account for differences in cell number. Data labeled with different letters are significantly different from each other (one-way ANOVA with Tukey's multiple comparisons, $p < 0.05$).

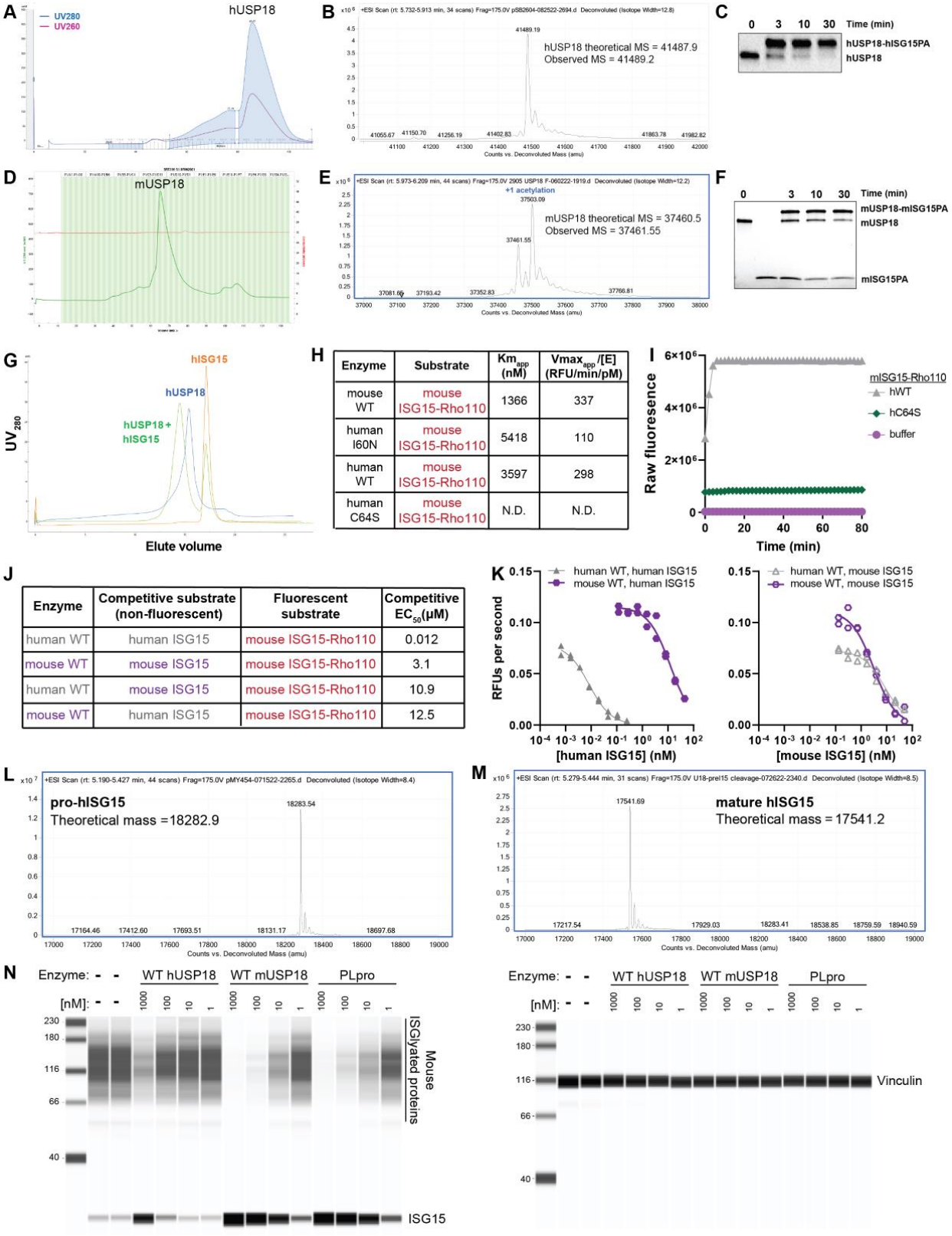


| Enzyme | Substrate | $Km_{app}$ (nM) | $Vmax_{app}$/[E] (RFU/min/pM) |
|---|---|---|---|
| mouse WT | mouse ISG15-Rho110 | 1366 | 337 |
| human I60N | mouse ISG15-Rho110 | 5418 | 110 |
| human WT | mouse ISG15-Rho110 | 3597 | 298 |
| human C64S | mouse ISG15-Rho110 | N.D. | N.D. |

| Enzyme | Competitive substrate (non-fluorescent) | Fluorescent substrate | Competitive $EC_{50}$(μM) |
|---|---|---|---|
| human WT | human ISG15 | mouse ISG15-Rho110 | 0.012 |
| mouse WT | mouse ISG15 | mouse ISG15-Rho110 | 3.1 |
| human WT | mouse ISG15 | mouse ISG15-Rho110 | 10.9 |
| mouse WT | human ISG15 | mouse ISG15-Rho110 | 12.5 |

**Figure S3. hUSP18 exhibits limited catalytic activity towards hISG15 substrate, related to Figure 3.** (A-F) Recombinant hUSP18 and mUSP18 were assessed for sample purity and quality. (A, D) hUSP18 and mUSP18 were purified by Ni-affinity chromatography and size exclusion chromatography. (B, E) Observed molecular weight was confirmed by mass spectrometry. (C, F) 50 nM hUSP18 (C) or 1 µM mUSP18 (F) was incubated with 5000 nM human ISG15-PA (hISG15PA) probe (C) or 10 µM mouse ISG15-PA (mISG15PA) probe (F) at $37^0$C for 30 min prior to assessing conjugation by western blot (C) or SDS-PAGE gel (F). (G) 50 µM hUSP18 was incubated with or without 75 µM hISG15 at RT for 5 min prior to assessing complex formation by size exclusion chromatography. (H) $K_{M(apparent)}$ and $V_{MAX(apparent)}$/[Enzyme concentration] determinations for hUSP18 (WT, I60N, or C64S) or mUSP18 vs mISG15-Rho110. The reported values are averaged from 2 determinations at different enzyme concentrations and rounded to 2 significant digits. N.D. = Not determined; signal below level of detection. (I) Progression curve of 1000 nM mISG15-Rho110 cleavage by 10 nM hUSP18 (WT or C64S) or no enzyme control (buffer) at RT. (J, K) Non-fluorescent hISG15 or mISG15 was added at the indicated concentration to 1 µM mISG15-Rho110 (Ac-ISG15prox-Rh110MP) and 1 nM hUSP18 or 2 nM mUSP18, respectively. Changes in fluorescence upon addition of non-fluorescent substrate were used to determine competitive $EC_{50}$ values. (L, M) Cleavage of 5 µM pro-hISG15 (AA1-165) to mature hISG15 (AA1-157) was assessed by mass spectrometry after 10 min incubation at $37^0$C with 1 µM of recombinant human WT hUSP18. (N) CT26 *mUsp18* KO cells were treated for 24 h with IFN-α prior to cell lysis and lysates were incubated with 1, 10, 100, or 1000 nM of indicated recombinant protein for 1 h at RT. Lysates were analyzed by western blot for levels of ISGylated proteins and mISG15 (left) or vinculin (right).

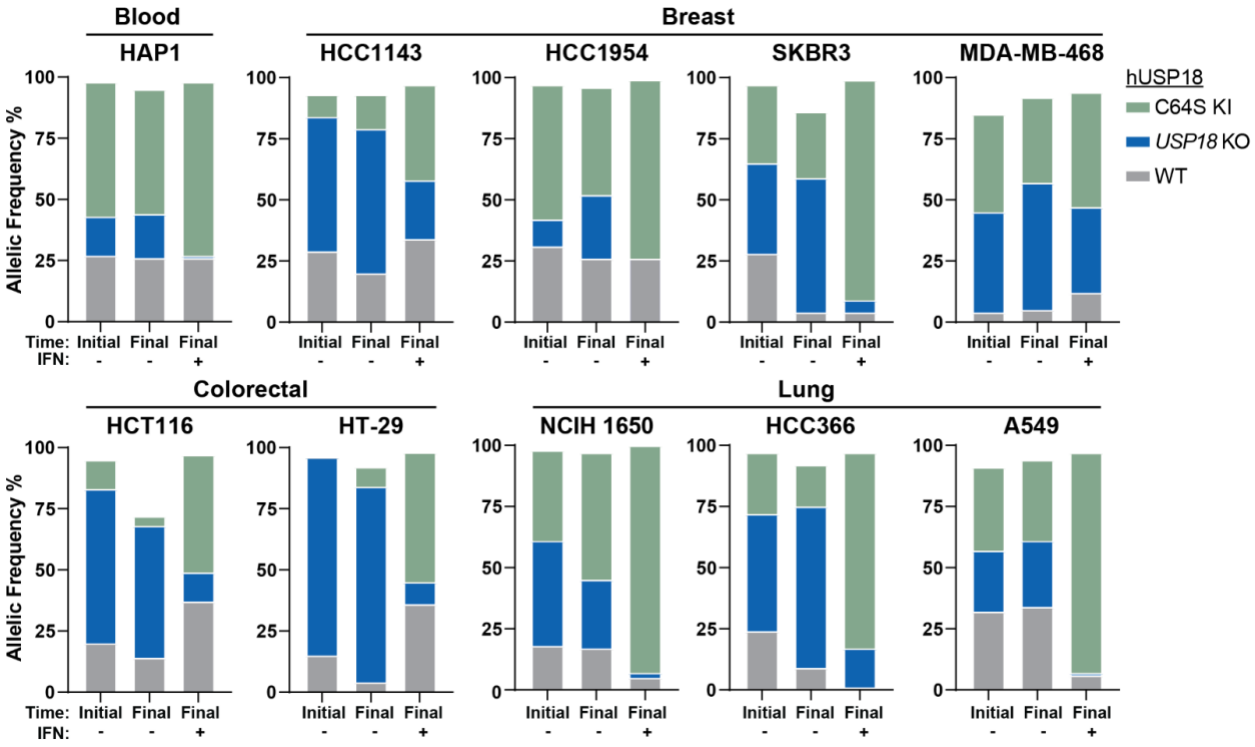


**Figure S4. Cancer cells expressing hUSP18 C64S are not sensitive to IFN, related to Figure 6.** Independent biological replicate run in parallel with Figure 6: parental human cancer cell lines were electroporated with C64S donor oligo and sgRNA targeted to *hUSP18*. Allelic frequency was

determined by sequencing samples 72 h post-electroporation (time initial) and after 2 additional weeks of passaging cells (time final) in the presence (+) or absence (-) of 1000 U/mL IFN-α. KO indicates frame-shift mutation or in-frame mutation ≥ 21 bp; WT indicates no mutation or in-frame mutation < 21 bp; KI indicates donor oligo integration at the intended position.

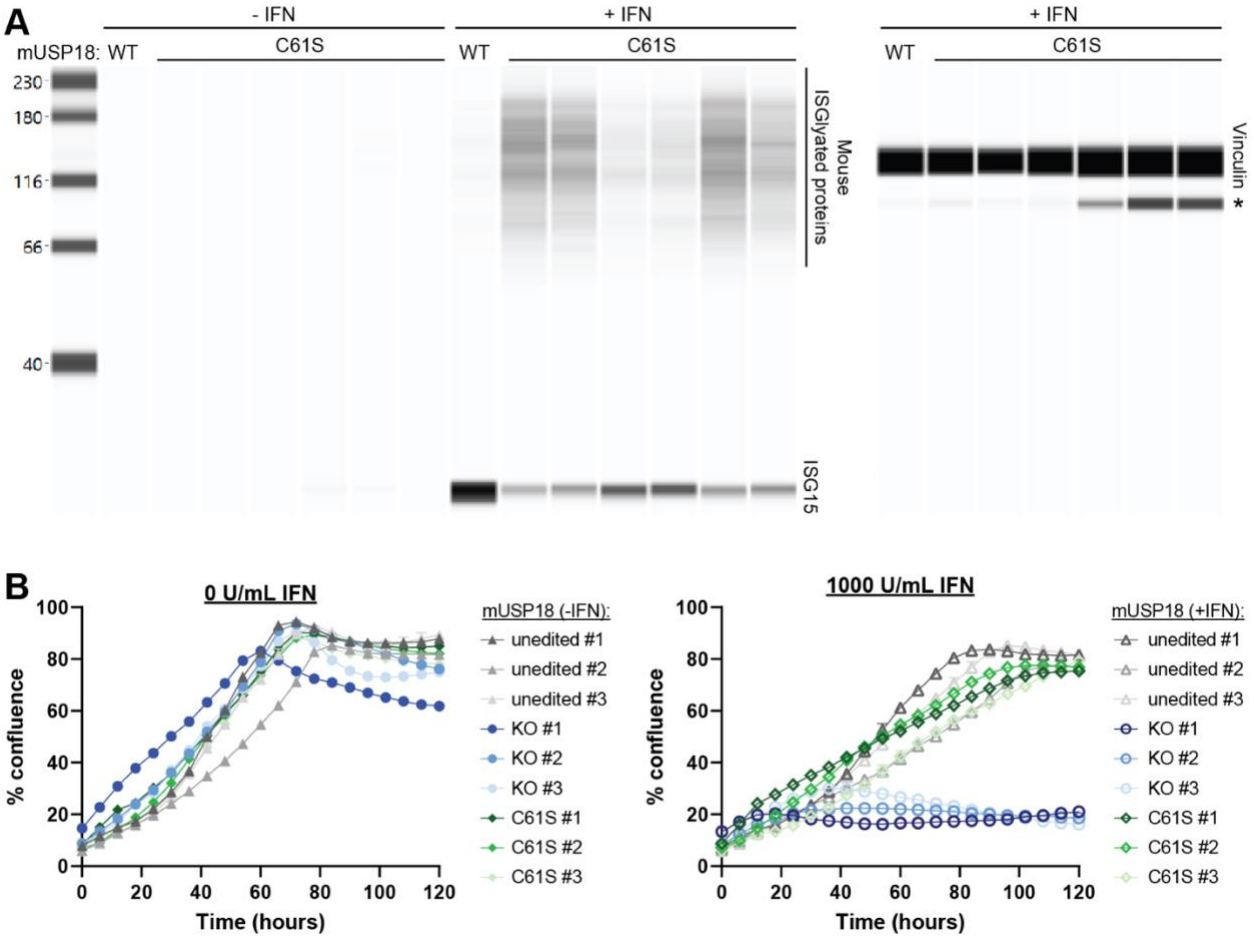


**Figure S5. Mutations in mUSP18 catalytic activity are not sufficient to confer IFN sensitivity in vitro, related to Figure 7.** Individual unedited control (unedited), mUSP18 C61S KI (C61S), and *mUsp18* KO (KO) clones were compared to parental CT26 cells (WT). Unedited control clones underwent same electroporation conditions as C61S KI and KO clones, but no editing was observed at the endogenous *mUsp18* locus. (A,B) Independent experiments from Figure 7A, 7B. (A) Cells were treated with 1000 U/mL murine IFN-α for 24 h prior to cell lysis and whole cell lysates were analyzed by western blot for levels of mouse ISGylated proteins and free mISG15 (left, all samples) or vinculin (right, +IFN samples only). * indicates non-specific band. (B) Growth rate ± 1000 U/mL murine IFN-α added at time = 0 hours. Each data point denotes mean of n = 2 replicates ± SEM. $EC_{50}$ determinations for each cell line are presented in Table S1. From left to right, C61S clone # in (A) is denoted as the following order in (B): #1, #2, #5, #4, #3, #6. Clones #1, #2, and #3 were selected for the in vivo study because these clones exhibited the largest increase in ISGylation, which could correlate with inhibition of catalytic activity.

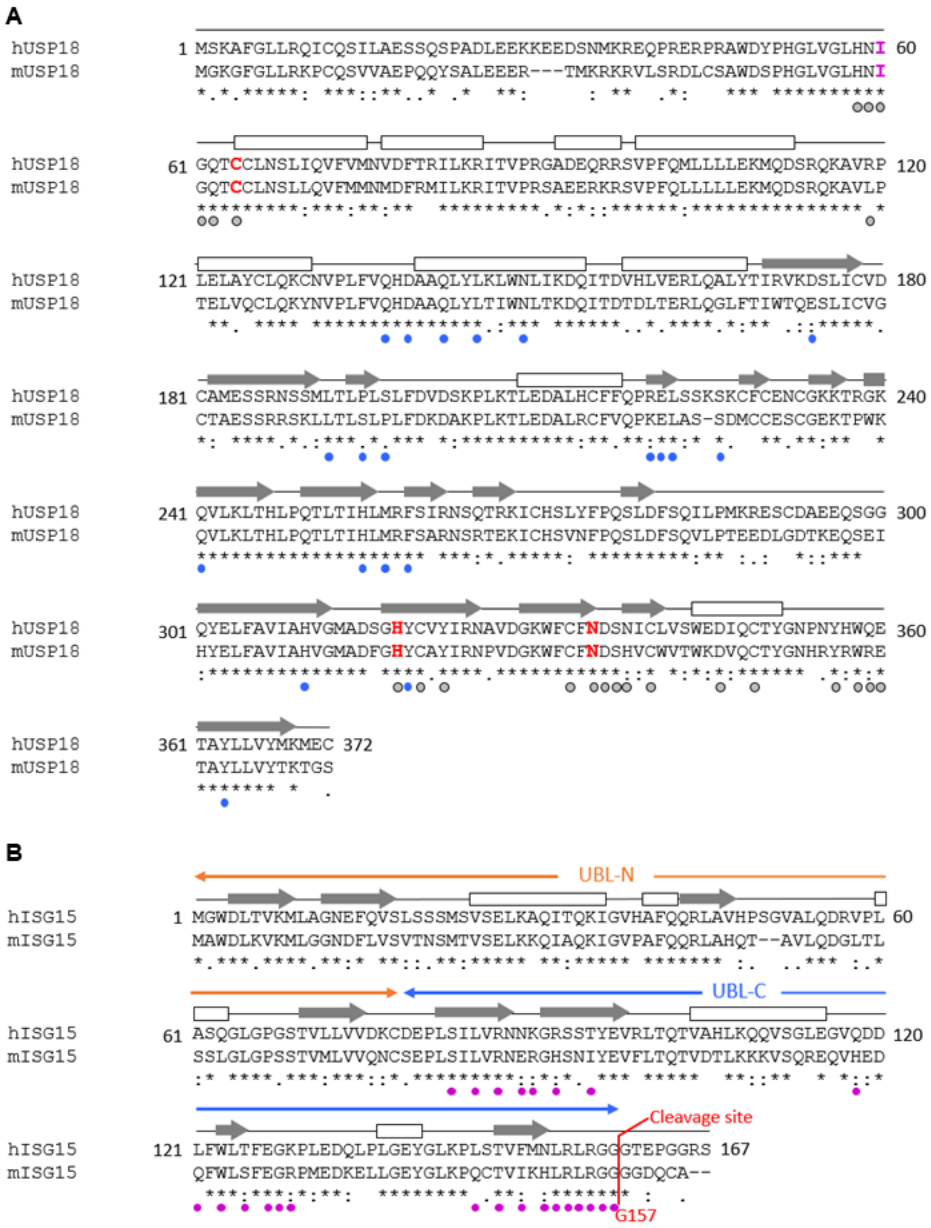


**Figure S6. Sequence alignments of hUSP18 vs mUSP18 and hISG15 vs mISG15, related to Figure 7.** (A,B) Sequences of hUSP18 vs mUSP18 and hISG15 vs mISG15 were aligned using CLUSTAL W. Open boxes and shared arrows below aligned sequences indicate α-helix and β-sheet secondary structure, respectively. (A) Human USP18 (top) aligned to mouse USP18 (bottom). Magenta and red amino acids indicate I60 and catalytic triad, respectively. Blue and gray circles below aligned sequences indicate predicted interface with human ISG15 and human STAT2, respectively. (B) Human ISG15 (top) aligned to mouse ISG15 (bottom). Orange and blue arrows above aligned sequences indicate N- and C-terminal ubiquitin-like (Ubl) domains, respectively. Magenta circles below aligned sequences indicate predicted interface with hUSP18. Cleavage of pro-ISG15 to mature ISG15 occurs at G157 (red).

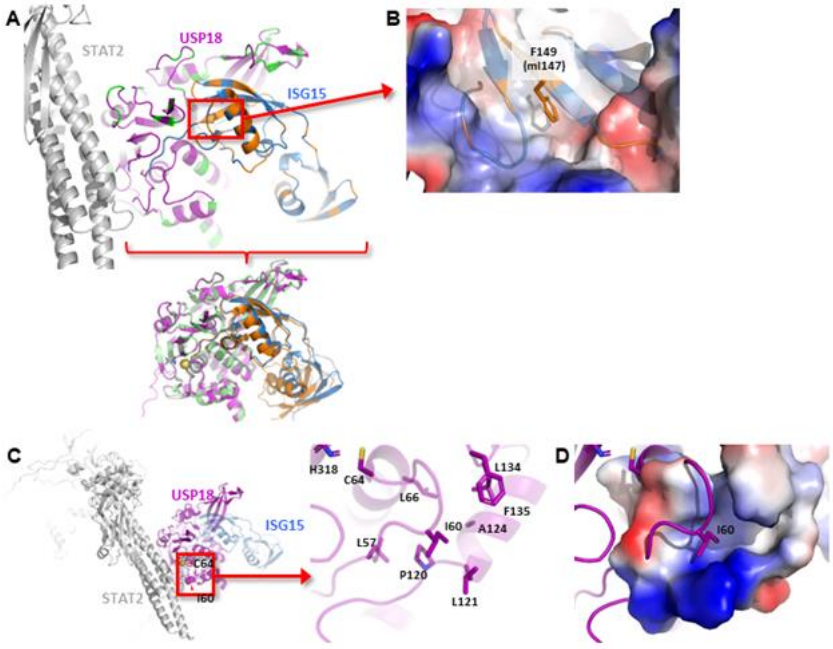


**Figure S7. USP18-ISG15-STAT2 interactions may be important for USP18 catalytic and scaffold function, respectively, related to Figure 7.** (A,C) Tertiary structure model of human USP18 (magenta), human ISG15 (blue), and STAT2 (gray) predicted by AlphaFold. (B, D) Surface electrostatic potential of USP18. Red, blue, and white indicate negative, positive, and neutral (hydrophobic), respectively. (A) Sequence differences between hUSP18 and mUSP18 (light green) or hISG15 and mISG15 (orange) were mapped onto the hUSP18-hISG15 structure in the AlphaFold ternary complex model using PyMOL. RMSD = 0.498 Å. (B) As an example, hISG15 F149 differs from mISG15 I147, which may impact hydrophobic interactions and contribute to species-specific binding affinities between USP18-ISG15. (C) human USP18 I60 is located near the USP18-STAT2 interface. (D) Altered hydrophobic interactions upon hUSP18 I60N mutation may cause conformational changes and/or fluctuations that disrupt USP18-STAT2 interactions.